Computational Energy Science

Vol. 2, No. 3, p. 93-97, 2025

Original article

Frequency-dependent morphological evolution of a liquid drop under AC electric fields

Fang Xiong[1], Xinyue Liu[1], Yuze Zhang[2], Lei Wang[1]*

[1]*School of Mathematics and Physics, China University of Geosciences, Wuhan 430074, P. R. China*

[2]*School of Mathematical Sciences, Ministry of Education key Laboratory of NSLSCS, Nanjing Normal University, Nanjing 210023, P. R. China*

Keywords:
Alternating current
electrohydrodynamics
lattice Boltzmann method
droplet deformation

Cited as:
Xiong, F., Liu, X., Zhang, Y., Wang, L. Frequency-dependent morphological evolution of a liquid drop under AC electric fields. Computational Energy Science, 2025, 2(3): 93-97.
https://doi.org/10.46690/compes.2025.03.02

Abstract:
The electrohydrodynamics of droplets driven by alternating current electric fields involves complex competition between charge relaxation and fluid inertia. To investigate this non-equilibrium process, this paper employs a thermodynamically consistent phase-field Lattice Boltzmann Method coupled with the Nernst-Planck equation to numerically simulate the dynamic response and morphological evolution of leaky dielectric droplets under alternating current (AC) electric fields. This study systematically decouples the hydrodynamic response from the competition of electrohydrodynamic stresses. First, in a baseline scenario where conductivity and permittivity act cooperatively, three frequency-dependent dynamic regimes are revealed: a quasi-steady breathing mode at low frequencies, a resonant oscillation mode at medium frequencies, and a steady-state saturation mode at high frequencies. Second, in a competitive scenario where conductive and dielectric stresses oppose each other, the AC frequency is found to act as a "switch" controlling the equilibrium shape of the droplet. As the frequency increases, the dominant mechanism shifts from a conductivity-driven regime caused by free charge accumulation to a permittivity-driven regime resulting from dielectric polarization. This shift leads to a morphological transition from prolate to oblate, with a dynamic balance achieved at a critical crossover frequency. This research elucidates the regulatory mechanism of AC frequency on droplet transient evolution and morphology, providing a theoretical basis for precise droplet manipulation in microfluidic systems.

1. Introduction

In frontier fields such as micro/nanofluidics (Agnihotri et al., 2025), optofluidics (Cheng et al., 2025) and precision biochemical detection (Xing et al., 2024), the precise non-contact manipulation of microdroplets using external electric fields has emerged as a core technology (Jiang et al., 2024). Compared to traditional mechanical or thermal actuation methods, electrohydrodynamic (EHD) technology can directly induce electric stresses at the fluid interface, thereby efficiently controlling droplet morphology, transport, and fission behaviors (Basaran et al., 2013). With advantages including rapid response, high integration, and strong programmability, this technology has demonstrated broad prospects in applications such as variable-focus liquid lenses (Ren and Wu, 2013), electronic paper display technologies, and high-throughput microdroplet screening (Link et al., 2006).

To accurately predict these complex electrohydrodynamic processes, establishing a rigorous theoretical model is an indispensable prerequisite. While the classic Taylor's leaky dielectric model laid the foundation for steady-state droplet behaviors (Melcher and Taylor, 1969), its simplified assumptions neglect charge diffusion effects and the spatiotemporal evolution of ion concentration gradients, making it difficult to accurately describe the dynamic details of charge distribution in the bulk and at interfaces under non-equilibrium states. Recent work by Gañán-Calvo (2025) points out that for microscale flows driven by unsteady electric fields, traditional electrokinetic approximations often require refined scaling laws to

Yandy Scientific Press

*Corresponding author.
E-mail address: xiongfang2024@126.com (F. Xiong); liuxinyue@nudt.edu.cn (X. Liu); 05439@njnu.edu.cn (Y. Zhang); wangleir1989@126.com (L. Wang).

Received July 7, 2025; revised August 3, 2025; accepted September 4, 2025; available online September 9, 2025.

accurately capture charge transport mechanisms. Therefore, to more realistically reflect charge dynamic characteristics from a physical mechanism perspective, introducing a charge transport model based on Nernst-Planck flux has become the optimal choice (Luo et al., 2016). Recent numerical work by Pan et al. (2024) has further confirmed the rigor and stability of this model in capturing charge relaxation behaviors with finite rates.

This refined consideration of the finite time characteristics of charge relaxation is particularly critical in alternating current (AC) electric field scenarios. As noted by Saville (1997), droplet dynamics under AC electric fields are essentially the result of the competition between the external field frequency and the charge relaxation frequency. The pioneering work of Torza et al. (1971) first laid the theoretical foundation for this field, revealing the intrinsic correlation between AC field parameters and droplet deformation. Subsequent theoretical derivations (Torza et al., 1971; Sozou, 1972) and classic experimental studies (Xu et al., 2023; Bono et al., 2024) have further confirmed that the synergistic action of electric field amplitude and frequency can significantly alter the spatiotemporal distribution of interfacial electric stresses, thereby inducing distinct evolutionary laws in droplets. Based on these physical mechanisms, current research efforts have shifted towards achieving on-demand customization of droplet dynamic behaviors through the precise regulation of AC parameters (Wang et al., 2025), satisfying the growing manipulation demands of microfluidic systems (Wang et al., 2024).

Given the limitations of analytical methods in handling nonlinear coupling, numerical simulation has become crucial for EHD research. The Lattice Boltzmann Method (LBM) is widely favored for its superiority in managing complex interfacial topology and convection-diffusion problems (Krüger et al., 2017). In this study, we adopt the thermodynamically consistent phase-field LBM framework developed by Xiong et al. (2025). By rigorously integrating the Nernst-Planck equation, this model accurately captures charge transport and dynamic interfacial evolution, providing a robust foundation for our simulations.

While steady-state behaviors under direct current (DC) fields are well-documented (Melcher and Taylor, 1969; Feng, 1999), the transient dynamics under alternating current (AC) fields-specifically the response governed by the competition between fluid inertia and charge relaxation-remain underexplored. Consequently, this paper utilizes the aforementioned framework to systematically investigate the influence of AC frequency on droplet deformation. By analyzing the cooperative and competitive mechanisms of conductive and dielectric stresses, we aim to elucidate the transient evolution mechanisms, offering theoretical insights for optimizing AC electro-controlled systems.

2. Problem setup and nondimensional parameters

The schematic of the problem configuration is illustrated in Fig. 1. The computational domain consists of a square cavity. Initially, a circular droplet of radius r is centered within the cavity and suspended in a surrounding medium. An electric field is established by grounding the bottom wall and applying an oscillating electric potential to the top wall, defined as (Esmaeeli and Halim, 2018):

$$\varphi(x,0,t) \equiv \varphi_b \equiv 0, \quad \varphi(x,L,t) \equiv \varphi_t \equiv \varphi_0 \sin(\omega t) \tag{1}$$

where φ_0 denotes the amplitude of the alternating electric field and ω represents the angular frequency. Consequently, in the absence of the droplet, the applied background electric field intensity is given by $E(t) = E_0 \sin(\omega t)$, where $E_0 = \varphi_0/L$. Regarding boundary conditions, periodic boundary conditions are applied in the horizontal direction, while the no-slip boundary conditions at the top and bottom plates are implemented using the half-way bounce-back scheme (Krüger et al., 2017).

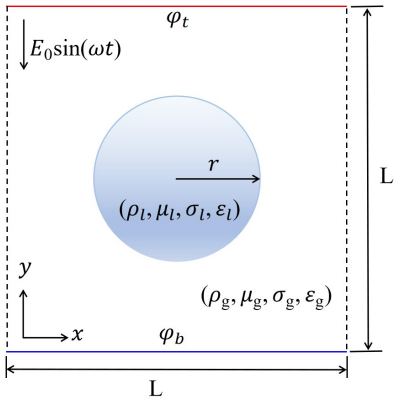

Fig. 1. The configuration of a droplet suspended in another leaky dielectric fluid under a uniform electric field. The subscripts l and v represents the internal and external fluids, respectively.

The physical properties of the fluids include densities ρ_l, ρ_g, viscosities μ_l, μ_g, dielectric constants ε_l, ε_g, and electrical conductivities σ_l, σ_g. The surface tension is denoted by γ. The subscripts l and g refer to the liquid droplet (inner phase) and the ambient medium (outer phase), respectively. The dimensionless control parameters governing the system are defined as follows:

$$\begin{aligned} &\mathrm{Re} = \frac{r^2 \rho_g \varepsilon_g E_0^2}{\mu_g^2}, \quad \mathrm{Re}_E = \frac{\varepsilon_g^2 E_0^2}{\mu_g \sigma_g}, \quad \alpha = \frac{\widetilde{\omega} k_B T \mu_g}{\varepsilon_g r^2 E_0^2} \\ &Ca = \frac{\mu_l v r}{\gamma}, \quad Ca_E = \frac{\varepsilon_l E_0^2 r}{\gamma} \end{aligned} \tag{2}$$

where Re is the Reynolds number defined as the ratio of electric force to viscous force, Re_E is the electric Reynolds number used to quantify the surface charge convection, α is the charge diffusion coefficient with k_B, $\widetilde{\omega}$ and T being the Boltzmann constant, charge mobility and fluid temperature, respectively.

In all simulations presented in this study, the width of the square domain is set to $L = 8r$, and the lattice size of the computational domain is fixed at 200×200. To eliminate the influence of buoyancy on droplet migration, simulations are conducted using density-matched fluids ($\rho_l = \rho_g$). Other parameters utilized in the phase-field simulation are selected

as follows: γ = 0.001 (surface tension), W = 5.0 (interface width), and M = 0.1 (mobility). Furthermore, to ensure that charge transport within the system is dominated by the Ohmic conduction mechanism rather than convection, a sufficiently small electric Reynolds number (i.e., $Re_E < 1$) is selected. Based on relevant experimental data, the Reynolds number is of the order $O(1)$, and the charge diffusion coefficient is approximately 10^{-4}. Based on the aforementioned analysis, unless otherwise specified, all subsequent simulations in this section are performed under the conditions of $Re_E = 10^{-3}$, Re = 1.0, $\alpha = 10^{-4}$, and Ca_E = 0.2.

3. Mathematical formulation and numerical method

In this study, the system is assumed to consist of immiscible and incompressible Newtonian fluids. The fluid dynamics are governed by the Navier-Stokes equations, while the electric field is described by the electrostatic equations coupled with the Nernst-Planck equation for charge transport (Xiong et al., 2025):

$$\nabla \cdot \mathbf{u} = 0 \tag{3}$$

$$\rho\left(\frac{\partial \mathbf{u}}{\partial t} + \mathbf{u}\cdot\nabla\mathbf{u}\right) = -\nabla p + \nabla\cdot\left[\mu(\nabla\mathbf{u} + \nabla\mathbf{u}^T)\right] + \mathbf{F}_s + q\mathbf{E} \tag{4}$$

$$\nabla\cdot(\varepsilon\mathbf{E}) = q, \quad \mathbf{E} = -\nabla\varphi \tag{5}$$

$$\frac{\partial q}{\partial t} + \mathbf{u}\cdot\nabla q = \nabla\cdot(\alpha\nabla q + \sigma\nabla\varphi) \tag{6}$$

where $\mathbf{u}$, p, ρ, and μ represent the fluid velocity, pressure, density, and dynamic viscosity, respectively; $\mathbf{E}$ and q denote the electric field strength and space charge density; ε, σ, and α represent the dielectric permittivity, electrical conductivity, and charge diffusion coefficient. $\mathbf{F}_s$ is the surface tension force. The interfacial evolution is tracked using the phase-field method via the Cahn-Hilliard equation (Xiong et al., 2025):

$$\begin{aligned} &\frac{\partial \phi}{\partial t} + \mathbf{u}\cdot\nabla\phi = \nabla\cdot M\nabla\mu_\phi \\ &\mu_\phi = 4\beta\phi(\phi-1)(\phi-0.5) - \kappa\nabla^2\phi - \frac{1}{2}\varepsilon'(\phi)|\mathbf{E}|^2 \end{aligned} \tag{7}$$

where ϕ is the order parameter (0 for the light fluid and 1 for the heavy fluid), M is the mobility, and μ_ϕ is the chemical potential including the electric stress term. The parameters β and κ are related to the surface tension γ and the interface width W. The physical properties (ρ, μ, σ, ε) are interpolated across the interface using standard linear or Hermite schemes as detailed in Xiong et al. (2025).

To solve the aforementioned coupled macroscopic equations, this study employs the lattice Boltzmann method (LBM) with a two-dimensional nine-velocity lattice structure and the single-relaxation-time (SRT) Bhatnagar-Gross-Krook (BGK) collision operator. The numerical solution schemes for the four physical fields–flow field, phase field, electric potential, and charge density (including the evolution equations, equilibrium distribution functions, and source term treatments)–strictly follow the computational framework established in Xiong et al. (2025).

4. Result and discussion

In this section, we investigate the dynamic behavior and morphological evolution of a leaky dielectric droplet under an AC electric field $E(t)$. To systematically decouple the effects of hydrodynamic response and EHD force competition, we analyze two distinct representative cases. We first examine the baseline scenario (R = 5, S = 60), where both conductivity and permittivity ratios favor prolate deformation, to isolate the hydrodynamic frequency response. Subsequently, we extend the analysis to a competitive scenario (R = 5, S = 0.5), where the conductive and dielectric forces act in opposition, highlighting the frequency-dependent shape transition (Torza et al., 1971; Saville, 1997).

Focusing first on the hydrodynamic dynamics, simulations were conducted for the baseline case (R = 5, S = 60) at three characteristic time periods: T = 120,000 Δt (Low Frequency), T = 80,000 Δt (Medium Frequency), and T = 4,000 Δt (High Frequency). As illustrated in Fig. 2, the droplet exhibits three distinct dynamic regimes determined by the ratio of the electric field period to the characteristic hydrodynamic response time. In the low-frequency limit (T = 120,000 Δt), the period of the external driving force is significantly longer than the hydrodynamic relaxation time. Consequently, the fluid responds instantaneously to the electric stress variations. The droplet undergoes a "quasi-steady breathing" mode, where it elongates to its maximum deformation at the field peak and fully retracts to a spherical shape ($D \approx 0$) as the field crosses zero, indicating that inertial effects are negligible in this regime (Feng and Scott, 1996; Esmaeeli and Sharifi, 2011). As the frequency increases to the medium range (T = 80,000 Δt), the driving period becomes comparable to the hydrodynamic response time, and fluid inertia begins to play a dominant role. In this resonant regime, the droplet exhibits large-amplitude oscillations. However, unlike the low-frequency case, the droplet fails to recover its spherical shape during the zero-field crossing ($D_{min} > 0$). Before the droplet can fully relax, the electric field in the subsequent half-cycle increases and pulls it apart again. A distinct phase lag is also observed between the deformation peak and the electric field peak, signifying substantial viscous dissipation (Mandal and Chakraborty, 2017). Conversely, in the high-frequency limit (T = 4,000 Δt), the field oscillates much faster than the fluid can respond. The viscous damping effectively filters out the high-frequency components of the electric stress, causing the droplet to respond only to the time-averaged RMS force (Saville, 1997). Consequently, the deformation parameter stabilizes at a constant value with negligible fluctuations, behaving similarly to a droplet in an equivalent DC electric field.

While the analysis of the baseline case elucidates the temporal response of the fluid, it represents a scenario of "cooperative" stresses where the equilibrium shape remains qualitatively unchanged across frequencies. However, in many practical applications involving composite fluids, the conductive and dielectric properties may exert competing forces. To capture the more complex physics where frequency dictates not just the stability but the direction of deformation, we must

consider the scenario where these forces act in opposition. We therefore introduce the competitive case (R = 5, S = 0.5). In this configuration, the conductivity ratio (R = 5) favors prolate elongation, whereas the permittivity ratio (S = 0.5) favors oblate compression. This setup allows the AC frequency to act as a decisive "switch" between two distinct physical mechanisms: Charge relaxation and dielectric polarization.

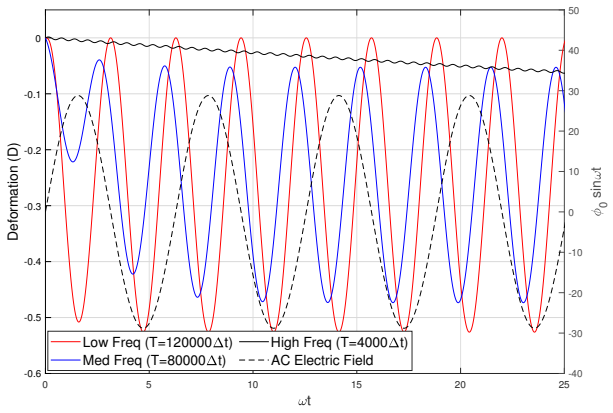

Fig. 2. Evolution of the deformation parameter D with time at different frequencies, and the applied voltage.

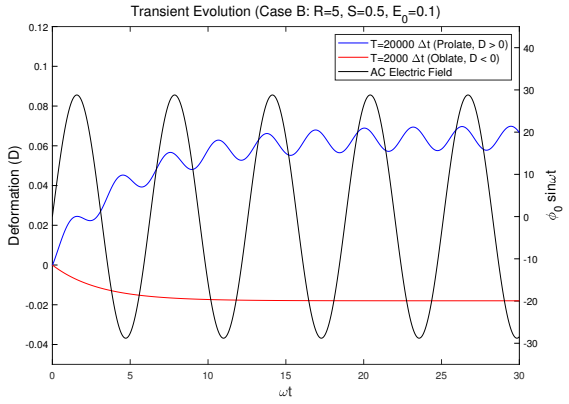

Fig. 4. Evolution of the deformation parameter D with time.

As depicted in Figs. 3 and 4, the droplet in this competitive scenario undergoes a distinct shape transition from prolate to oblate as the frequency increases (Torza et al., 1971). In the low-frequency range ($T \geq$ 80,000 Δt), the time scale is sufficient for free charges to migrate and accumulate at the interface. Since R = 5, the fluid behaves as a leaky conductor. The tangential migration of free charges generates an extensional stress that elongates the droplet ($D > 0$), consistent with the behavior observed in DC electric fields (Melcher and Taylor, 1969). In this regime, the conductivity mismatch dominates the EHD interaction. However, as the frequency increases towards the high-frequency limit ($T \leq$ 400 Δt), the rapid oscillation of the electric field prevents free charges from accumulating at the interface. Consequently, the droplet behaves as a perfect dielectric, and the electric stress is governed solely by the polarization mismatch. Dominated by the permittivity ratio S = 0.5, the polarization stress compresses the poles and stretches the equator, resulting in an oblate deformation ($D < 0$). Between these two extremes, there will be a crucial crossover frequency at which the electrical (pulling force) and dielectric (pushing force) stresses dynamically balance each other (Vlahovska, 2019). At this specific frequency, the time-averaged deformation parameters approach zero, enabling the droplet to maintain a nearly spherical shape even in the presence of a strong electric field.

5. Conclusion

This study numerically investigates the frequency-dependent dynamics and morphological evolution of a leaky dielectric droplet under an AC electric field. By systematically decoupling the hydrodynamic response from electro-hydrodynamic stress competition, we identified three distinct dynamic regimes determined by the ratio of the electric field period to the fluid relaxation time. At low frequencies, the droplet follows a quasi-steady breathing mode with negligible inertia, whereas intermediate frequencies trigger resonant oscillations with significant phase lag. Conversely, high-frequency viscous damping suppresses oscillations, leading to a steady-state deformation governed by the time-averaged electric force.

Furthermore, in systems with competing electrical properties, the AC frequency acts as a decisive control parameter for droplet morphology. As frequency increases, a morphological transition from prolate to oblate occurs, shifting the dominance from conductivity-driven charge accumulation to permittivity-driven polarization. Consequently, the droplet transitions from a leaky conductor to a perfect dielectric. A critical crossover frequency was also identified where these opposing stresses dynamically balance, maintaining the droplet in a near-spherical equilibrium despite the strong electric field.

Acknowledgements

This work is financially supported by the National Natural Science Foundation of China (Grants No. 12301554 and No. 12472297).

Conflict of interest

The authors declare no competing interest.

References

Agnihotri, S. N., Raveshi, M. R., Nosrati, R., et al. Droplet splitting in microfluidics: A review. Physics of Fluids, 2025, 37(5): 051304.

Basaran, O. A., Gao, H., Bhat, P. P. Nonstandard inkjets. Annual Review of Fluid Mechanics, 2013, 45(1): 85-113.

Bono, S., Kinugasa, H., Kajita, H., et al. Resonant oscillation of droplets under an alternating electric field to enhance solute diffusion. Scientific Reports, 2024, 14(1): 21326.

Cheng, G., Kuan, C., Lou, K., et al. Light-responsive materials

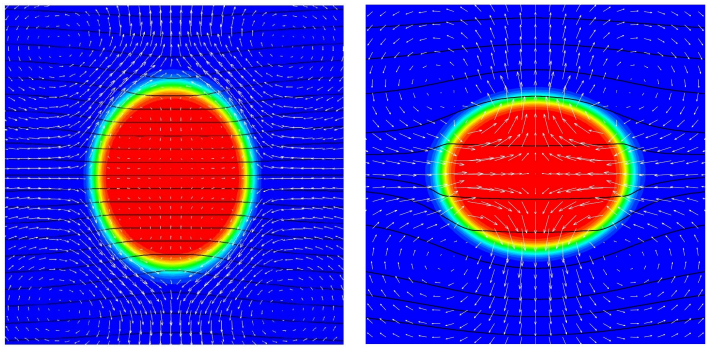

(a) (b)

Fig. 3. Transient evolution of the deformation parameter D for the competitive scenario (R = 5, S = 0.5, E_0 = 0.1) at different frequencies. The black dashed line represents the electric potential.

in droplet manipulation for biochemical applications. Advanced Materials, 2025, 37(2): 2313935.

Esmaeeli, A., Halim, M. A. Electrohydrodynamics of a liquid drop in AC electric fields. Acta Mechanica, 2018, 229(9): 3943-3962.

Esmaeeli, A., Sharifi, P. Transient electrohydrodynamics of a liquid drop. Physical Review E-Statistical, Nonlinear, and Soft Matter Physics, 2011, 84(3): 036308.

Feng, J. Q. Electrohydrodynamic behaviour of a drop subjected to a steady uniform electric field at finite electric Reynolds number. Proceedings of the Royal Society of London. Series A: Mathematical, Physical and Engineering Sciences, 1999, 455(1986): 2245-2269.

Feng, J., Scott, T. C. A computational analysis of electrohydrodynamics of a leaky dielectric drop in an electric field. Journal of Fluid Mechanics, 1996, 311: 289-326.

Gañán-Calvo, A. M. The spatial structure of jets from steady Taylor cone-jets. Journal of Fluid Mechanics, 2025, 1023: A49.

Jiang, Y., Yang, L., Ye, D., et al. Modeling and analysis of jetting behavior of surface charge-induced electrohydrodynamic printing. Physics of Fluids, 2024, 36(10): 102002.

Krüger, T., Kusumaatmaja, H., Kuzmin, A., et al. The lattice Boltzmann method, Springer International Publishing 10(978-3) (2017) 4-15

Link, D. R., Grasland-Mongrain, E., Duri, A., et al. Electric control of droplets in microfluidic devices. Angewandte Chemie-International Edition in English, 2006, 45(16): 2556.

Luo, K., Wu, J., Yi, H., et al. Lattice Boltzmann model for Coulomb-driven flows in dielectric liquids. Physical Review E, 2016, 93(2): 023309.

Mandal, S., Chakraborty, S. Effect of uniform electric field on the drop deformation in simple shear flow and emulsion shear rheology. Physics of Fluids, 2017, 29(7): 072109 .

Melcher, J. R., Taylor, G. I. Electrohydrodynamics: A review of the role of interfacial shear stresses. Annual review of fluid mechanics, 1969, 1(1): 111-146.

Pan, M., Liu, S., Zhu, W., et al. A linear, second-order accurate, positivity-preserving and unconditionally energy stable scheme for the Navier-Stokes-Poisson-Nernst-Planck system. Communications in Nonlinear Science and Numerical Simulation, 2024, 131: 107873.

Ren, H., Wu, S. Variable-focus liquid lens by changing aperture. Applied Physics Letters, 2005, 86(21): 211107.

Saville, D. Electrohydrodynamics: The Taylor-Melcher leaky dielectric model. Annual Review of Fluid Mechanics, 1997, 29(1): 27-64.

Sozou, C. Electrohydrodynamics of a liquid drop: The time-dependent problem. Proceedings of the Royal Society of London. A. Mathematical and Physical Sciences, 1972, 331(1585): 263-272.

Torza, S., Cox, R. G., Mason, S. G. Electrohydrodynamic deformation and bursts of liquid drops. Philosophical Transactions of the Royal Society of London. Series A, Mathematical and Physical Sciences, 1971, 269(1198): 295-319.

Vlahovska, P. M. Electrohydrodynamics of drops and vesicles. Annual Review of Fluid Mechanics, 2019, 51(1): 305-330.

Wang, D., Chagot, L., Wang, J., et al. Effect of electric field on droplet formation in a co-flow microchannel. Physics of Fluids, 2025, 37(2): 023331.

Wang, G., Chen, W., Chen, J., et al. Mechanism of the pinch-off electrohydrodynamic printing breaking through the characteristic frequency limit. Journal of Fluid Mechanics, 2025, 1015: A58.

Wang, W., Vahabi, H., Taassob, A., et al. On-demand, contactless and loss-less droplet manipulation via contact electrification. Advanced Science, 2024, 11(10): 2308101.

Xing, Y., Wang, Y., Li, X., et al. Digital microfluidics methods for nucleic acid detection: A mini review. Biomicrofluidics, 2024, 18(2): 021501.

Xiong, F., Wang, L., Huang, J., et al. A thermodynamically consistent phase-field lattice Boltzmann method for two-phase electrohydrodynamic flows. Journal of Scientific Computing, 2025, 103(1): 1-32.

Xu, W., Huo, L., Zhao, Y., et al. Breakup of a leaky dielectric droplet in a half-sinusoidal wave electric field. Chemical Engineering Research and Design, 2023, 197: 96-108.